FACILE FUNCTIONALIZATION OF sp^2 CARBON ALLOTROPES WITH A BIOBASED *JANUS* MOLECULE

M. GALIMBERTI,* V. BARBERA, S. GUERRA, A. BERNARDI

POLITECNICO DI MILANO, DEPARTMENT OF CHEMISTRY, MATERIALS AND CHEMICAL ENGINEERING "G. NATTA," VIA MANCINELLI 7, 20131 MILANO, ITALY

RUBBER CHEMISTRY AND TECHNOLOGY, Vol. 90, No. 2, pp. 285–307 (2017)

ABSTRACT

A simple, versatile, sustainable, not expensive method for the functionalization of sp^2 carbon allotropes, both nano-sized and nano-structured, without altering their bulk crystalline organization, is presented. Carbon materials available at the commercial scale were used: furnace carbon black (CB), nano-sized graphite with high surface area, and multiwalled carbon nanotubes. A bio-sourced molecule, 2-(2,5-dimethyl-1*H*-pyrrol-1-yl)-1,3-propanediol (serinol pyrrole), was used for the functionalization. Serinol pyrrole (SP) was obtained from serinol through a reaction with atomic efficiency of about 82%, performed in the absence of solvents or catalysts. Synthesis of serinol pyrrole was performed as well on carbon allotropes as the solid support. Adducts of serinol pyrrole with a carbon allotrope were prepared with the help of either thermal or mechanical energy. Functionalization yield was in all cases larger than 90%. With such adducts, stable dispersions in water and in NR latex were prepared. A few layers of graphene were isolated from the water dispersions, and NR-based composites precipitated from the latex revealed very even distribution of fine graphitic particles. Composites were prepared, based on NR, IR, and BR as the rubbers and CB and silica as the fillers, with different amounts of CB–SP adduct, and were cross-linked with a sulfur-based system without observing appreciable effect of functionalization on vulcanization kinetics. The CB–SP adduct led to appreciable reduction of the Payne effect. [doi:No. 10.5254/rct.17.82665]

INTRODUCTION

In the field of rubber, Charles Goodyear's pronouncement "There is probably no other inert substance the properties of which excite in the human mind an equal amount of curiosity, surprise and admiration"[1] is well known. He was referring to natural rubber, indeed a fascinating material, which, however, could not be used for important applications, even after cross-linking. To achieve important mechanical properties, natural and synthetic rubbers need reinforcing fillers.[2] Indeed, carbon black (CB)[3–4] and silica,[5] the so-called nano-structured fillers, are largely used for the mechanical reinforcement of rubbers. They are made by primary nanometric particles, fused together to form micron-sized aggregates. Over the last decades, nano-fillers have appeared on the rubber scene,[6–8] and they have attracted great interest. In fact, they can be separated in individual nanometric particles and can establish large interfacial area with the polymer matrix, with great impact on the material properties. Most investigated nano-fillers are clays and organo clays (OC),[6–11] carbon nanotubes (CNT),[6–8,12] and graphene (G) or graphite nano-platelets made by few layers graphene.[13–17] Nano-fillers can not completely replace CB and silica in rubber compounds. However, very interesting results have been reported by using hybrid filler systems such as CB–OC, CB–CNT, and CB–G,[18] and synergistic effects have been demonstrated. In particular, research is steadily increasing on filler systems based on CNT and graphene, thanks to their exceptional properties.

Recently, the focus of research is on sp^2 carbon allotropes. It is even amazing how many new allotropes have been obtained over the last years, most of them with nano-dimensions.[19] It could be assumed that there is no room for new carbon materials. Instead, it has been recently reported[20] that various new allotropes have yet to be synthesized. Major challenges are seen in "combining low-

*Corresponding author. Email: maurizio.galimberti@polimi.it

dimensional forms into more complex 3D architectures" and much work is, in particular, expected "to develop and optimize applications of nanotubes and graphene."

By looking at such a multitude of sp^2 carbon allotropes as potential fillers for rubber composites, two basic questions arise: (i) Is it possible to rationalize their behavior, identifying filler features able to establish common correlation with the composite properties? (ii) Should sp^2 carbon allotropes be used as such, or should they be modified upon introducing functional groups? Answers to such questions can be attempted, as follows.

Need is increasing for a common rationalization of the behavior of carbon fillers, in polymer and in particular rubber composites. Nano-size and nano-structured carbon fillers have been so far separately investigated in most scientific works. Recent studies have compared crystallinity, shape anisotropy, density, surface area, and oil absorption of CNT, a nano-sized graphite and CB.[21,22] Synergistic effects have been demonstrated in thermoplastic[15] and elastomeric matrices.[17,18,22–25] Interestingly, correlation has been established between the initial modulus of composites based on CNT, CB or the hybrid filler system, and the filler–polymer interfacial area: a master curve was elaborated, obtaining the fitting of the experimental points.[17,18,22] The specific interfacial area also has been demonstrated to correlate parameters of the sulfur-based cross-linking of natural rubber, such as induction time (t_{s1}) and activation energy, in the presence of CNT, a nano-sized graphite with high surface area and CB: master curves were reported.[26]

It is increasingly acknowledged that to achieve substantial improvement of properties and to enlarge the span of applications, carbon materials should be functionalized. An impressive amount of scientific literature is available. Supramolecular and covalent modification of CNT has been performed,[27–29] achieving stable dispersions in different solvents, water, and latexes; improving compatibility with polymer matrices; generating polymers on CNT surfaces (grafting from polymerizations); and preparing a large variety of devices. Use of functionalized CNT in rubber composites is not yet much explored. Supramolecular modification is preferred: for example, ionic liquids were used to achieve low electrical percolation threshold in chloroprene rubber.[30] Indeed, CNTs are considered (rightly or wrongly) expensive materials, and their functionalization is not expected to solve this problem. Functionalization of graphene layers is a hot research topic.[31–37] The use of exfoliated graphene oxide platelets allowed stable and fine dispersions in natural rubber (NR) latex and interconnected graphene networks in the nano-composites.[38,39] Relevant efforts have been dedicated to the functionalization of carbon black, both in the academic and industrial worlds.[40–48] At the industrial level, cofuming technology led to carbon/silicon dual phase;[41–42] CB was treated with ozone,[43–46] triazole,[47] and polysulfide.[48] The common objective of such technologies was to promote the interaction of CB with the polymer matrix.

The particular aim of the functionalization of carbon allotropes is the introduction of oxygenated groups. Oxidation of graphene layers to graphene oxide (GO) and subsequent reduction is considered the best way for large-scale preparation of graphene. Moreover, CB with OH groups could be reactive with sulfur-based silanes and then with rubber, through vulcanization. Reports on carbon oxidation date back to the 19th century. Most of the methods are based on harsh and even dangerous reaction conditions: The methods of Brodie,[49] Staudenmeier,[50] and Hummers[51] require the use of substances such as HNO_3 with $KClO_3$, H_2SO_4/HNO_3 with $KClO_3$, $H_2SO_4/NaNO_3$ with $KMnO_4$, respectively. Much research has been performed in order to improve the Hummers' method,[52–57] removing $NaNO_3$,[53] using H_2SO_4/H_3PO_4 mixture,[52] pre-oxidizing graphite with P_2O_5 and $K_2S_2O_8$ in H_2SO_4,[56] and playing with $NaNO_3$ and $KMnO_4$ concentration and residence times.[55] GO was also prepared by mechanochemical oxidation of graphite.[57] In order to obtain graphene from GO, the reduction step has been extensively studied, with hydrazine,[58–61] with hydrogen plasma,[60] with a base (NaOH 0.1 M) at moderate temperatures (80 °C),[62] with ascorbic acid,[63] and with a stabilizing agent to avoid reaggregation of graphitic flakes.[64] Thermal[66]

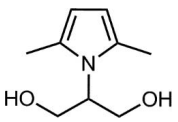

FIG. 1. — 2-(2,5-dimethyl-1*H*-pyrrol-1-yl)-1,3-propanediol (SP).

and flash[67] reductions have been reported. However, reduction is incomplete, and the ideal graphitic structure is not preserved.[68,69]

The research here reported had the aim to develop a simple, versatile, sustainable, not expensive method, which can introduce functional groups on both nano-size and nano-structured sp^2 carbon allotropes, using carbon materials available at the commercial scale. The particular objective was to preserve the bulk structure of the graphitic materials by introducing functional groups in peripheral positions of the graphene layers. Recently, the most challenging task for the functionalization of graphene layers is indeed the selective introduction of functional groups at the layers' edges. This manuscript reports on the introduction of oxygenated functional groups. Functionalization was performed by using the molecule shown in Figure 1: 2-(2,5-dimethyl-1*H*-pyrrol-1-yl)-1,3-propanediol (serinol pyrrole [SP]).

SP derives from glycerol, a cheap, easily available chemical, nontoxic and biodegradable, the main by-product of bio-diesel production.[70–72] In particular, a glycerol derivative with enhanced chemoselectivity was used for the one pot reaction that led to SP: 2-amino-1,3-propandiol (serinol, S). Serinol is a commercially available substance: it is prepared from glycerol or dihydroxyacetone and it can also be obtained from renewable sources.[73]

The following topics are reported: synthesis of SP neat and on a carbon allotrope (CA) as the solid support; preparation of SP adducts with CB, high surface area graphite (HSAG), and CNT; and preparation of dispersions in water and NR latex of such adducts and of rubber compounds based on NR, IR, and butadiene rubber (BR) and on CB and/or silica as the fillers. This paper is mainly focused on carbon allotrope functionalization, and preliminary data on rubber-based compounds are discussed. Adducts of SP with carbon allotropes were characterized by means of solvent extraction, thermogravimetric analysis (TGA), Raman spectroscopy, wide angle X-ray diffraction (WAXD), and Fourier transformed infrared spectroscopy (FT-IR). Dispersions in water of CA–SP adducts were studied through dynamic light scattering (DLS) and ultraviolet–visible (UV–Vis) analyses. HSAG isolated from the water dispersion was characterized with high-resolution transmission electron microscopy (HRTEM). The structure of NR-based composites was studied with TEM and WAXD analyses. Rubber compounds cross-linking was studied by means of rheometric analysis, and filler networking was investigated with strain sweep measurements in the shear mode.

EXPERIMENTAL

MATERIALS

For the Synthesis of Serinol Pyrrole. — Reagents and solvents commercially available were purchased and used without further purification: 2,5-hexandione (Merck–Schuchardt, Hohenbrunn, Germany), 2-amino-1,3-propandiol (kindly provided by Bracco SPA, Milan).

Rubbers. — The synthetic poly(1,4-*cis*-isoprene) (IR) used had the trade name SKY3 from Nizhnekamskneftekhim Export (Nizhnekamsk, Russia), with 70 Mooney Units (MU) as Mooney viscosity (M_L(1+4)100 °C); the synthetic poly (1,3-butadiene) (BR) used had the trade name neocis BR 40 from Versalis (San Donato Milanese, Italy), with a 43 Mooney Viscosity (M_L(1+4)100 °C);

TABLE I
SURFACE AREA, DBP ABSORPTION NUMBER, AND NUMBER OF GRAPHENE LAYERS STACKED IN CRYSTALLINE DOMAIN FOR sp^2 CARBON ALLOTROPES

Carbon allotrope	Surface area[a], m^2/g	DBP absorption number, mL/100 g[b]	Number of stacked layers[c]
HSAG	330	162	35
GnP	750	n.d.[d]	26
CNT[e]	275	316	9
CB N326[f]	77	85	5

[a] From BET measurements (see ref. 79).
[b] Milliliters of absorbed DBP/100 g of CB (see ref. 79).
[c] Estimated from WAXD pattern (see ref. 57).
[d] n.d. = not determined.
[e] Nanocyl 7000.
[f] From Cabot (Boston, MA, USA).

and the poly(1,4-cis-isoprene) from *Hevea brasiliensis* (NR) (EQR, E.Q. Rubber; Eastern Group, Chonburi, Thailand) had the trade name SIR20 and 73 Mooney Units (MU) as Mooney viscosity ($M_L(1+4)100\,°C$). Latex from *Hevea brasiliensis*: SIR20 from Chonburi, Eastern Group Thailand.

Carbon Allotropes. — Carbon black N326 (CB) was from Cabot, with the following characterization data: 30 nm as mean diameter of spherical primary particles. Multiwall carbon nanotubes (MWCNT) were NANOCYL® NC7000™ series, with carbon purity of 90% and average length of about 1.5 μm. High surface area graphite (HSAG) was Nano24 from Asbury Graphite Mills Inc. (Kittanning, PA, USA), with carbon content reported in the technical data sheet of at least 99 wt%. Chemical composition determined from elemental analysis was, as wt%: carbon 99.5, hydrogen 0.4, nitrogen 0.1, oxygen 0.0. Graphene nano-platelets (GnP) were purchased from Sigma Aldrich (St. Louis, MO, USA). For all the carbon allotropes, surface area, dibutyl phthalate (DBP) absorption number, and number of layers stacked in crystalline domain are reported in Table I.

For Dispersion Preparation. — Acetone and ethyl acetate (Aldrich) were used as received.

For Rubber Compound Preparation. — Silica was Zeosil 1115 (industrial grades for tire applications) from Solvay (Brussels), with 115 m^2/g as specific surface area determined through nitrogen absorption (Brunauer-Emmett-Teller [BET]). The following ingredients were used as received: bis(3-triethoxysilylpropyl) tetrasulfide (TESPT) (Si69 Evonik, Essen, Germany), ZnO (zinc oxide), Stearic acid (Sogis, Cremona, Italy), (1,3-dimethyl butyl)-*N*′-Phenyl-p-phenylenediamine (6PPD) (Crompton, Middlebury, CT, USA), sulfur (Solfotecnica, Cotignola, Italy), *N*-*tert*-butyl-2-benzothiazyl sulfenamide (TBBS), *N*-cyclohexyl-2-benzothiazyl sulfenamide (CBS) (Flexsys, Ann Arbor, MI, USA).

SYNTHESIS OF SERINOL PYRROLE

Synthesis of 2-(2,5-dimethyl-1H-pyrrol-1-yl)-1,3-propanediol (SP). — A mixture of 2,5-hexandione (37.67 g; 0.33 mol) and serinol (30.06 g; 0.33 mol) was poured into a 100 mL round bottomed flask equipped with magnetic stirrer. The mixture was then stirred, at room temperature, for 6 h. The resulting compound 4a,6a-dimethyl-hexahydro-1,4-dioxa-6b-azacyclopenta[*cd*]pentalene (HHP) was characterized through ^{1}H-NMR, and the yield was estimated to be 99%.

The product mixture obtained from the synthesis of HHP was kept under vacuum for 2 h and then heated to 180 °C for 60 min. After distillation under reduced pressure at 130 °C and 0.1 mbar,

SP was isolated as yellow oil with 96% yield.

^{1}H−NMR(400MHz, DMSO−d6, δin ppm) :
2.16(s, 6H, $-CH_3$at C − 2, 5 of pyrrole moiety); 3.63(m, 2H, CH_2OH); 3.76(m, 2H, CH_2OH);
4.10(quintet, 1H, at C − 3 of diol);4.73(t, 2H, CH_2OH);5.55(s, 2H, C − 3, 4 of pyrrole moiety).

SYNTHESIS OF SP WITH REAGENTS SUPPORTED ON HSAG AS THE CARBON ALLOTROPE

In a 50 mL round bottom flask equipped with magnetic stirrer were poured HSAG (0.2 g), serinol (0.084 g, 0.922 mmol), and 2,5-hexandione (0.105 g, 0.922 mmol). The mixture was stirred at 150 °C for 2 h. After this time the mixture was kept to room temperature and D_2O (2 mL) was added. The suspension was filtered using a polytetrafluoroethylene (PTFE) 0.2 micron. The liquid was analyzed by means of ^{1}H-NMR spectroscopy. SP was isolated as yellow oil after washing the black powder with water (90% yield).

SYNTHESIS OF SP WITH REAGENTS SUPPORTED ON CNT AS THE CARBON ALLOTROPE

In a 50 mL round bottom flask equipped with magnetic stirrer were poured MWCNT (0.2 g), serinol (0.084 g, 0.922 mmol), and 2,5-hexandione (0.105 g, 0.922 mmol). The mixture was stirred at 150 °C for 2 h. After this time the mixture was kept to room temperature and D_2O (2 mL) was added. The suspension was filtered using a PTFE 0.2 micron. The liquid was analyzed by means of ^{1}H-NMR spectroscopy. SP was isolated as yellow oil after washing the black powder with water (86% yield).

SYNTHESIS OF SP WITH REAGENTS SUPPORTED ON CB N326 AS THE CARBON ALLOTROPE

In a 50 mL round bottom flask equipped with magnetic stirrer were poured CB N326 (0.2 g), serinol (0.084 g, 0.922 mmol), and 2,5-hexandione (0.105 g, 0.922 mmol). The mixture was stirred at 150 °C for 2 h. After this time the mixture was kept to room temperature and D_2O (2 mL) was added. The suspension was filtered using a PTFE 0.2 micron. The liquid was analyzed by means of ^{1}H-NMR spectroscopy. SP was isolated as yellow oil after washing the black powder with water (82% yield).

SYNTHESIS OF sp^2 CARBON ALLOTROPES ADDUCTS

Carbon allotrope adducts with SP (CA–SP) were prepared starting from mixtures of CA and SP and donating them either mechanical (CA–SP–M) or thermal (CA–SP–T) energy. Preparations of adducts with HSAG are reported as examples.

GENERAL PROCEDURE FOR MECHANICAL TREATMENT: HSAG–SP–M ADDUCT

In a 100 mL round bottomed flask was put in sequence HSAG (5 g, 66 mmol) and acetone (15 mL). The suspension was sonicated for 15 min, using a 2 L ultrasonic bath. After this time, a solution of SP (5.87 g, 66 mmol) in acetone (15 mL) was added. The resulting suspension was sonicated for 15 min. The solvent was removed under reduced pressure. The black powder of HSAG/SP was treated using a planetary ball mill S100 from Retsch (Haan, Germany), having the grinding jar moving in a horizontal plane, with a volume of 0.3 L. The grinding jar was loaded with six ceramic balls having a diameter of 20 mm. HSAG/SP adduct (10.87 g) was put into the jar, which was allowed to rotate at 300 rpm, at room temperature, for 6 h. After this time, the mixture

was placed in a Büchner funnel with a sintered glass disc. It was repeatedly washed with distilled water (6 × 100 mL) obtaining 9.8 g of black powder.[74]

GENERAL PROCEDURE FOR THERMAL TREATMENT: HSAG–SP–T ADDUCT

In a 100 mL round bottom flask was put in sequence HSAG (5 g, 66 mmol) and acetone (15 mL). The suspension was sonicated for 15 min, using a 2 L ultrasonic bath. After this time, a solution of SP (1.116 g, 6.6 mmol) in acetone (15 mL) was added. The resulting suspension was sonicated for 15 min. The solvent was removed under reduced pressure. The black powder of HSAG/SP (6.10 g) was poured into a 100 mL round bottomed flask equipped with magnetic stirrer and was heated at 130 °C for 6 h. After this time, the mixture was placed in a Büchner funnel with a sintered glass disc. It was repeatedly washed with distilled water (3 × 20 mL), obtaining 5.86 g of black powder.[74]

DISPERSIONS OF CA–SP ADDUCTS

Water Dispersions. — Water dispersions of CB–SP adducts at different concentrations (1, 0.5, 0.3, and 0.1 mg/mL) were prepared. Each dispersion was sonicated for 10 min using an ultrasonic bath (260 W), and subsequently UV–Vis absorption was measured. The dispersion (10 mL) of each sample was put in a Falcon™ 15 mL conical centrifuge tube and centrifuged at 2000 rpm for 10 min and at 9000 rpm for 5, 30, 60, and 90 min. Supernatants obtained after each centrifugation process were removed and analyzed. UV–Vis absorptions and DLS analysis were measured immediately after each centrifugation and after 1 week storage.

Ethyl Acetate CNT Dispersion. — Ethyl acetate dispersions of CNT–SP adducts at concentration of 1 g/L were prepared. Each dispersion was sonicated for 10 min using an ultrasonic bath (260 W), and subsequently UV–Vis absorption was measured. The dispersion (10 mL) of each sample was put in a Falcon 15 mL conical centrifuge tube and centrifuged at 9000 rpm for 5 min. Supernatants obtained after each centrifugation process were removed and analyzed. UV–Vis absorptions and DLS analysis were measured immediately after sonication and centrifugation.

Dispersion of HSAG–SP Adduct in Natural Rubber Latex. — The natural rubber used was poly(1,4-*cis*-isoprene) from *Hevea brasiliensis*. HSAG–SP adduct (0.05 g) was added to 10 ml of water. The dispersion was then sonicated in a 2 L ultrasonic bath with a power of 260 Watts for 15 min. A dispersion was obtained, in which no presence of powders was noted. This dispersion was added to 0.84 g of latex. The dispersion obtained was stirred with magnetic stirrer for 60 min and then sonicated for 1 min. Precipitation was then performed by adding a 0.1 M sulfuric acid solution. A composite material based on natural rubber containing HSAG was obtained.

Dispersion of CB–SP in Natural Rubber Latex. — The natural rubber used was poly(1,4-cis-isoprene) from *Hevea brasiliensis*. CB–SP adduct (0.05 g) was added to 10 mL of water. The dispersion was then sonicated in a 2 L ultrasonic bath with a power of 260 Watts for 15 min. A solution was obtained, in which no presence of powders was noted. This solution was added to 0.84 g of latex. The dispersion obtained was stirred with magnetic stirrer for 60 min and then sonicated for 1 min. Precipitation was then performed by adding a 0.1 M sulfuric acid solution. A homogeneous and continuous composite material based on natural rubber containing carbon black was obtained.

Centrifugation of Water Dispersions of CA–SP Adducts. — Water suspensions (1 g/L) of adducts were centrifuged using an ALC–Centrifugette 4206. Conditions for centrifugation are reported above and below in the text.

TABLE II
RECIPES OF COMPOSITES WITH CB–SP, CONTAINING IR, BR AS THE RUBBERS AND CB, SILICA AS THE FILLERS[a]

Ingredients	phr	phr	phr
IR	50.0	50.0	50.0
BR	50.0	50.0	50.0
CBN326	25.0	20.0	17.5
CB–SP[b]	0.0	5.0	7.5
Silica	25.0	25.0	25.0
TESPT	4.0	4.0	4.0

[a] Other ingredients (phr): ZnO 4.0, Stearic acid 2.0, S 1.5, 6PPD 2.0, CBS 1.8.
[b] Amount of SP on CB: 12 mass%.

PREPARATION OF CA–SP RUBBER COMPOUNDS

Rubber Compounds Based on IR, BR as Rubbers and CB and Silica as Fillers. — Recipes are in Table II and Table III.

Without CB–SP. — Poly(1,3-butadiene) (BR) (16.12 g) and poly(1.4-*cis*-isoprene) (IR) (16.12 g) were fed into a Brabender® (South Hackensack, NJ, USA) internal mixer with a mixing chamber with a volume of 50 cc and masticated at 145 °C for 1 min. Silica (8.06 g) and silane TESPT (1.09 g) were added and mixed for 4 min. The obtained compound was unloaded at 145 °C. The composite thus prepared was then fed into the internal mixer at 80 °C, masticated for 1 min, then 8.06 g of CB N326 were added and mixed for a further 4 min, then unloaded at 80 °C. This composite was fed again into the internal mixer at 50 °C, adding 1.29 g of ZnO, 0.64 g of stearic acid, and 0.64 g of 6PPD and mixed for 2 min. Sulfur (0.48 g) and *N*-cyclohexyl-2-benzothiazyl sulfenamide (CBS) (0.58 g) were then added, mixing for a further 2 min. The composite was unloaded at 50 °C.

With CB–SP. — The same procedure was followed, except that an amount of CB was replaced by the same amount of CB–SP (in the first case 1.58 g, in the second case 2.32 g).[74]

RUBBER COMPOUND BASED ON NR, WITH CARBON BLACK AS THE FILLER

Without CB–SP. — Poly(1,4-*cis*-isoprene) (29.39 g) was fed into a Brabender internal mixer with a mixing chamber with a volume of 50 cc and masticated at 80 °C for 1 min. TESPT (1.10 g) and carbon black CB N326 (10.29 g) was then added, mixed for a further 5 min, and the compound obtained was unloaded at 145 °C. The composite thus prepared was then fed into the internal mixer

TABLE III
RECIPES OF COMPOSITES WITH CB–SP, CONTAINING NR AS THE RUBBERS AND CB AS THE FILLER[a,b]

Ingredients	phr	phr
NR	100	100[c]
CB N326	45	45[c]
SP	0	4[c]

[a] Amount of ingredients are expressed in phr.
[b] Other ingredients ZnO 5, Stearic acid 2, Sulfur 2, TBBS 1.
[c] NR–CB–SP master batch prepared from NR latex (see "Experimental" section).

at 80 °C, adding 1.47 g of ZnO and 0.59 g of stearic acid, and mixed for 2 min. Sulfur (0.66 g) and *N-tert*-butyl-2-benzothiazole sulfenamide (TBBS) (0.21 g) were then added, mixing for a further 2 min. The composite was unloaded at 90 °C.

With CB–SP. — The same procedure was followed, except that 10.29 g of CB–SP were added in place of 10.0 g of CB.

CHARACTERIZATION

Thermogravimetric Analysis. — TGA tests under flowing N_2 (60 mL/min) were performed with a Mettler TGA SDTA/851 (Columbus, OH, USA) instrument according to the standard method ISO9924-1. Samples (10 mg) were heated from 30 to 300 °C at 10 °C/min, kept at 300 °C for 10 min, and then heated up to 550 °C at 20 °C/min. After being maintained at 550 °C for 15 min, they were further heated up to 900 °C and kept at 900 °C for 30 min under flowing air (60 mL/min).

Elemental Analysis. — Elemental analysis was performed with a ThermoFlashEA 1112 Series CHNS-O analyzer, after pretreating samples in an oven at 100 °C for 12 h.

Fourier Transform Infrared. — FT-IR spectra were recorded between 450 and 4000 cm^{-1} by using a Perkin Elmer FT-IR Spectrum One (Waltham, MA, USA) equipped with Universal ATR Sampling Accessory with diamond crystal.

Raman Spectroscopy. — Raman spectra of powder samples deposited on a glass slide were recorded by using a Horiba (Edison, NJ, USA) Jobin Yvon Labram HR800 dispersive Raman spectrometer equipped with Olympus (Tokyo, Japan) BX41 microscope and a 50× objective. The excitation line at 632.8 nm of a He/Ne laser was kept at 0.5 mW in order to prevent possible samples degradation. The spectra were obtained as the average of four acquisitions (scan time: 30 s for each acquisition) with a spectral resolution of 2 cm^{-1}.

Wide Angle X-Ray Diffraction. — Wide-angle X-ray diffraction (WAXD) patterns were obtained in reflection, with an automatic Bruker (Billerica, MA, USA) D8 Advance diffractometer, with nickel filtered Cu–Kα radiation. Patterns were recorded in 10°–100° as the 2θ range, being 2θ the peak diffraction angle. Distance between crystallographic planes was calculated from the Bragg law. The $D_{hk\ell}$ correlation length, in the direction perpendicular to the $hk\ell$ crystal graphitic planes, was determined applying the Scherrer Eq. 1

$$D_{hk\ell} = K\lambda/(\beta_{hk\ell}\cos\theta_{hk\ell}) \quad (1)$$

where K is the Scherrer constant, λ is the wavelength of the irradiating beam (1.5419 Å, Cu-Kα), $\beta_{hk\ell}$ is the width at half height, and $\theta_{hk\ell}$ is the diffraction angle. The instrumental broadening, b, was determined by obtaining a WAXD pattern of a standard silicon powder 325 mesh (99%), under the same experimental conditions. The width at half height, $\beta_{hk\ell} = (B_{hk\ell} - b)$ was corrected, for each observed reflection with $\beta_{hk\ell} < 1°$, by subtracting the instrumental broadening of the closest silicon reflection from the experimental width at half height, $B_{hk\ell}$.[75]

UV–Vis Spectroscopy. — The suspensions of adduct (3 mL) were placed by pipette Pasteur, in quartz cuvettes of 1 cm optical path (volume 1 or 3 mL) and analyzed by a spectrophotometer Hewlett Packard (Palo Alto, CA, USA) 8452A Diode Array Spectrophotometer. The instrument was reset with pure solvent and has one UV spectrum from 200 to 340 nm. It was recorded as white with the solvent employed. The UV–visible spectrum reported the intensity absorption as a function of the wavelength of the radiation between 200 and 750 nm.

Dynamic Light Scattering. — The nanoparticle size in dispersions was analyzed with a Zetasizer Dynamic Light Scattering system (Malvern Instrument Ltd.) at room temperature using a l.25 mW 632.8 nm He–Ne laser. Each centrifuged dispersion, prepared using a concentration of 1 mg/mL, was analyzed by DLS: 3 mL of dispersion were placed using a pipette Pasteur, in a quartz

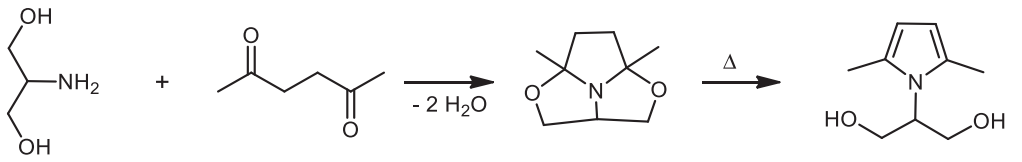

FIG. 2. — Paal–Knorr reaction between serinol and 2,5-hexanedione.

cuvette of 1 cm optical path, and analyzed immediately after centrifugation and after 10, 60, and 100 min of storage.

Transmission Electron Microscopy on HSAG–SP Sample from Water Dispersion. — TEM analysis of HSAG–SP adducts isolated from supernatant suspension was performed with a Zeiss EM900 microscope (Carl Zeiss AG, Oberkochen, Germany) operating at an accelerating voltage of 80 kV. Few drops of acetone diluted suspension of the sample were deposited on a carbon film supported on a standard Cu grid and air-dried for several hours before analysis.

High-Resolution Transmission Electron Microscopy on Adduct Samples. — HR–TEM investigations on adduct samples were carried out with a Zeiss Libra® 200 FE microscope (CNT–PU–SP sample) and with a Philips CM 200 field emission gun microscope (Philips, Amsterdam) operating at an accelerating voltage of 200 kV (HSAG–SP sample).

CNT–PU–SP sample (see Figure 12B) was isolated from the ethyl acetate suspension after centrifugation at 5000 rpm for 5 min. A few drops of ethyl acetate diluted suspension of the sample were deposited on a holey carbon film supported on a standard Cu grid and air-dried for several hours before analysis. HSAG–SP sample (see Figure 13A) was isolated from the supernatant water suspension after centrifugation at 9000 rpm for 5 min. A few drops of water suspension were deposited on 200 mesh lacy carbon-coated copper grid and air-dried for several hours before analysis.

Transmission Electron Microscopy on Rubber Composites. — Zeiss Libra 120 at an acceleration voltage of 120 kV was used with ultra-thin cryo-sections (100 nm) of rubber composites. The cryo-sections were prepared using an ultramicrotome cooled with liquid nitrogen (type: Reichert FC-4E Ultramicrotome, Depew, NY, USA) and diamond knives.

Cross-linking and Dynamic Mechanical Characterization of Rubber Compounds. — Cross-linking reaction was studied at 170 °C with a Monsanto RPA 2000 rheometer (Monsanto, St. Louis, MO, USA), determining the minimum modulud M_L, the maximum modulus M_H final at the end of cross-linking reaction, the time t_{s1} required to have a torque equal to M_{l+1}, and the time t_{90} required to achieve 90% of the maximum modulus M_H.

Dynamic shear moduli were then measured at 50 °C, with a sinusoidal strain at 1 Hz of frequency, in a strain amplitude ranging from 0.1% to 25%.

RESULTS AND DISCUSSION

SYNTHESIS OF 2-(2,5-DIMETHYL-1*H*-PYRROL-1-YL)-1,3-PROPANEDIOL (SP)

Serinol pyrrole was synthesized through the Paal–Knorr reaction[76,77] of 2-amino-1,3-propane diol with 2,5-hexanedione (HD). The reaction occurred through the pathway shown in Figure 2. S and HD were used in equimolar amount, and neat reaction was performed in the absence of solvents

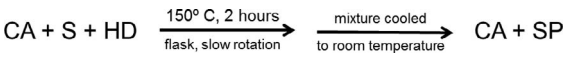

FIG. 3. — Process for the synthesis of serinol pyrrole on sp^2 CA.

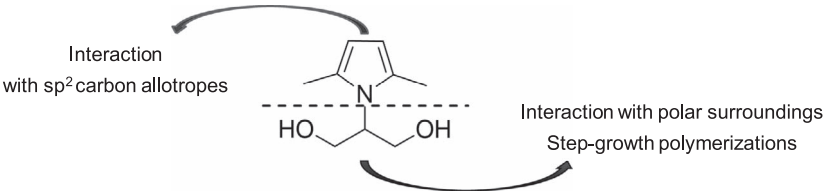

FIG. 4. — Serinol pyrrole: a Janus molecule able to interact with carbon allotropes and polar surroundings and to take part in step-growth polymerizations.

or catalysts.[78–81] Details are in the "Experimental" section. In brief, at room temperature the tricyclic intermediate 4a,6a-dimethyl-hexahydro-1,4-dioxa-6b-azacyclopenta[cd]pentalene, converted at high temperature in the aromatic compound, was obtained. Such reaction is characterized by high atom economy, 82.4%, the only by-product being water. Yield was found to be between 95% and 99%, and, therefore, the atom efficiency was from 78% to 82%. It is worth recalling that the Paal–Knorr reaction between S and HD was already reported in the literature,[82] in the presence of strong acids, obtaining a mixture of products and SP only as a by-product. It was thus unexpected[78] that the neat reaction, in the absence of an acidic catalyst (suggested for the Paal–Knorr reaction), could lead to such high yield. SP is a colorless liquid (light yellow before distillation), at room temperature and 1 atm pressure and has high solubility in water.

SYNTHESIS ON sp^2 CARBON ALLOTROPE AS SOLID SUPPORT

Serinol pyrrole was synthesized on sp^2 carbon allotropes, as described in detail in the experimental section. The process is summarized in Figure 3. The reaction product was extracted from the mixture with the carbon allotrope and was analyzed by ^{1}H-NMR analysis (in D_2O). Only SP was detected in the spectrum.

It was mentioned above that SP is obtained in the absence of solvents or catalysts. Results commented in this paragraph conclude that the synthesis can be also performed on a solid support, a carbon filler that will become part of the adduct with SP.

WHY TO USE SERINOL PYRROLE FOR FUNCTIONALIZING sp^2 CARBON ALLOTROPES

The Paal–Knorr reaction, performed on serinol as the substrate, leads to the formation of a pyrrole ring in place of the amino group: the hybridization of the nitrogen atom is changed from sp^3 to sp^2. SP becomes thus a Janus molecule, that is, a molecule with two physically or chemically differing faces.[83,84] Janus was a roman god, portrayed (e.g. in coins) with two faces in one body. Colloids,[85] block copolymers,[86] and proteins[87] can be Janus molecules. A Janus molecule is known to have a dual reactivity. The aromatic pyrrole ring could give rise to π–π stacking with aromatic compounds such as a carbon allotrope and could interact with lipophilic substances. The moiety that comes from glycerol, with the hydroxy groups, can establish interactions with polar environments.

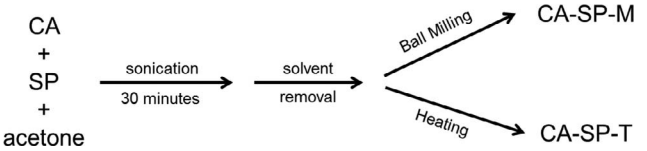

FIG. 5. — Procedure for the preparation of adducts of serinol pyrrole with a CA.

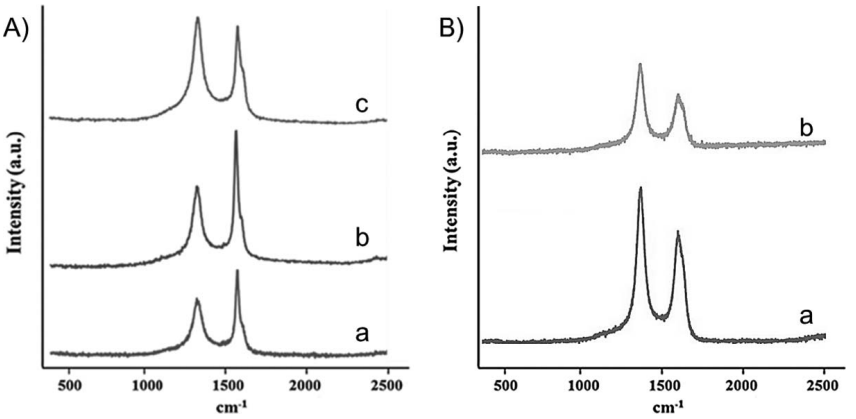

FIG. 6. — Raman spectra of (A) (a) HSAG, (b) HSAG–SP–M, (c) HSAG–SP–T; (B) (a) CNT, (b) CNT–SP.

Moreover, hydroxy groups can be suitable functional groups for the preparation of step-growth polymers.[79,81] SP as a Janus molecule is shown in Figure 4.

ADDUCTS OF SERINOL PYRROLE WITH sp^2 CARBON ALLOTROPES

The following carbon allotropes were used for the preparation of adducts with serinol pyrrole: high surface area graphite, multiwalled carbon nanotubes, carbon black. Their main characteristics are shown in Table I, and in the "Experimental" section.

The procedure for the preparation of adducts of SP with carbon allotropes is shown in Figure 5. Details are in the "Experimental" section. Adducts were prepared with the help of either thermal or mechanical energy, in the absence of solvents or any other chemical substance. In the text, they are indicated as CA–SP–M or CA–SP–T, where CA is HSAG, CNT, and CB.

The strength of interaction between SP and the carbon allotrope was investigated by performing Soxhlet extraction of the adducts with acetone (very good solvent for SP), weighing the sample before and after extraction, and/or taking the thermogravimetric analysis (TGA) on washed samples, detecting the mass loss between 250 °C and 500 °C.[80] The yield of functionalization was calculated through the following equation:

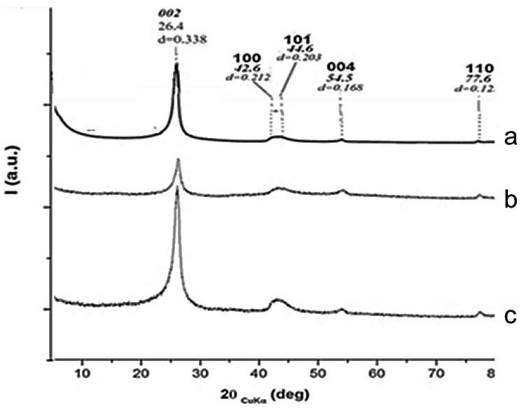

FIG. 7. — WAXD spectra of (a) HSAG, (b) HSAG–SP–M, (c) HSAG–SP–T.

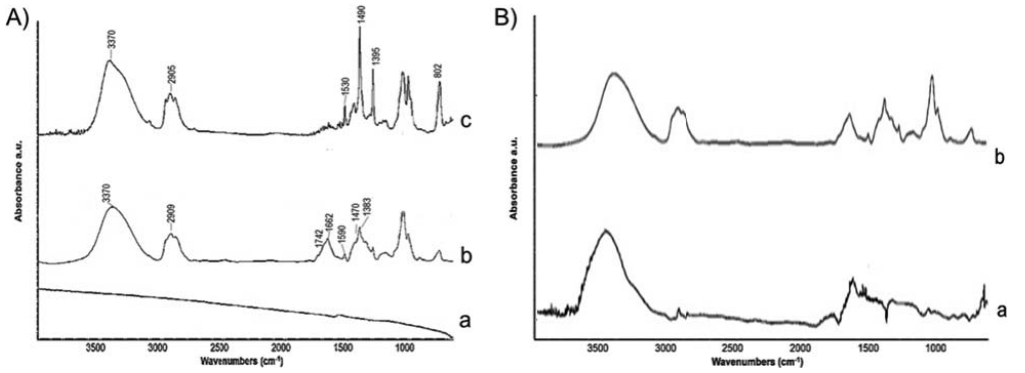

FIG. 8. — FT-IR spectra of (A) (a) HSAG, (b) HSAG–SP–T, and (c) SP;(B) (a) CB–SP, (b) HSAG–SP.

$$\text{Yield} = \frac{\text{SP in(CA} - \text{SP adduct)}_{\text{after the extraction}}}{\text{SP in(CA} - \text{SP adduct)}_{\text{before the extraction}}} 100 \quad (2)$$

In Table IV, the functionalization yield is reported for different carbon allotropes. High functionalization yields were obtained, at least 90%. Such a result suggests that SP is able to establish a very stable interaction with the carbon allotropes. This might lead to supposed modification, also to large extent, of the graphitic substrate. It was mentioned in the "Introduction" section that the main objective of this research was to preserve the bulk crystalline structure of the graphitic materials. WAXD and Raman analyses were thus performed on pristine carbon allotropes and on the adducts, to study their organization at the solid state. In the present work, results are shown with HSAG and CNT as the carbon allotropes.

In the Raman spectrum of carbonaceous material, lines named D and G and located at 1350 cm^{-1} and 1590 cm^{-1}, respectively, reveal the presence of graphitic sp^2-phase. The G peak is due to bulk crystalline graphite (graphene), whereas the D peak occurs in the presence of either disorder or confinement (e.g. by edges) of the graphitic layers.[88–92] Figure 6A shows the Raman spectra of (a) HSAG, (b) HSAG–SP–M, (c) HSAG–SP–T.

The D band is clearly visible in the spectrum of pristine HSAG. It has to be mentioned that HSAG is produced via milling: the high intensity of the D band can be thus attributed to the electronic perturbation of the crown region, confined close to the edge.[93] The relative intensity of the D and G bands appears substantially the same in pristine HSAG and in HSAG–SP–T, suggesting that the thermal treatment of HSAG with SP does not appreciably alter the HSAG structure. Instead, the intensity of the D band increases in HSAG–SP–M, after the mechanical treatment, which is likely to promote perturbation of the crystalline structure.

Raman analysis was also performed on CNT. Spectra shown in Figure 6B, of (a) pristine CNT and CNT–SP–T reveal features similar to the ones observed for HSAG in Figure 6A: both G and D

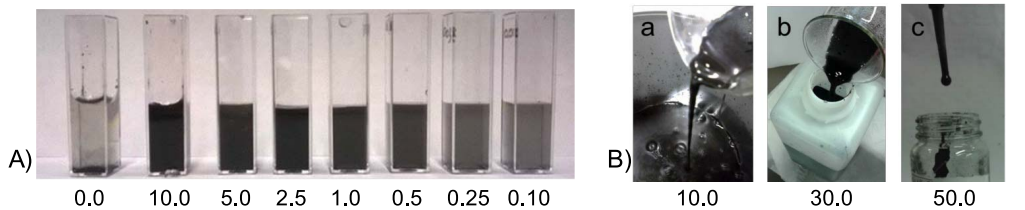

FIG. 9. — Water dispersions of HSAG. Concentrations (g/L) are indicated.

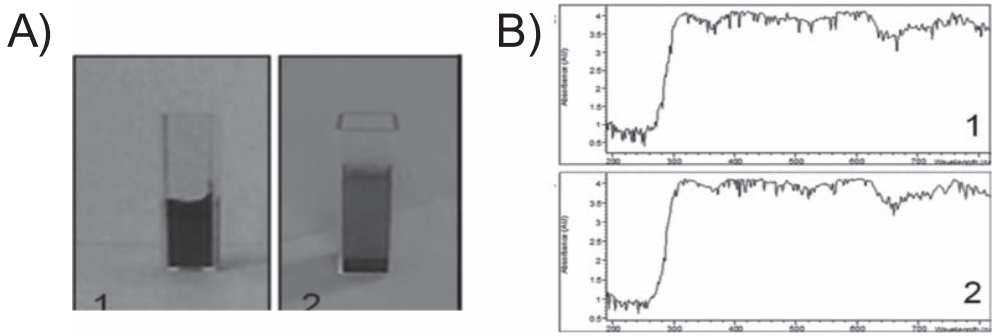

FIG. 10. — (A) Water dispersions of (1) CB–SP and of (2) CB, after centrifugation; (B) UV–Vis spectra of water suspensions of CB–SP adduct: (1) after sonication and (2) after centrifugation.

bands are visible in the spectrum of pristine CNT, and their relative intensity is not substantially altered by the thermal treatment with SP.

WAXD spectra of pristine HSAG and of the adducts are shown in Figure 7. The (002) reflection is at the same 2θ value in the three samples, indicating that SP is not intercalated in the interlayer space of HSAG. Peak shape analysis was performed by applying the Scherrer equation to the (002) reflection, estimating the number of layers stacked in a crystalline domain, which decreased from HSAG (35) to HSAG–SP–T (29) to HSAG–SP–M (24). The peak shape analysis of (100) and (110) reflections estimated a correlation length from 26.5 nm to 28 nm. This finding shows that neither the thermal nor the mechanical treatment substantially alter the in plane order of HSAG. It can be thus concluded that modification of HSAG with SP occurs essentially at the edges of the graphene layers.

FT-IR analysis was performed in order to investigate the nature of functional groups on the carbon allotropes. IR spectra of HSAG, HSAG–SP–T and SP, in the region between 700 cm^{-1} and 4000 cm^{-1} are reported in Figure 8A. In the spectrum of pristine HSAG (a), the peak visible at about 1590 cm^{-1} is attributed to the absorption of E_{1u} IR active mode of collective C=C stretching vibration of graphite/graphene materials. The diffusion/reflection phenomena of the IR beam passing through micro-particles of the carbonaceous material are responsible for the increasing background toward high wavenumbers. In the spectrum of SP (c), the broad bands at 3370 and at 2900 cm^{-1} could be attributed to hydrogen bonded OH groups and to C–H stretching due to methyl groups of the pyrrole ring and to methylene of the serinol moiety, respectively. Whereas bands at

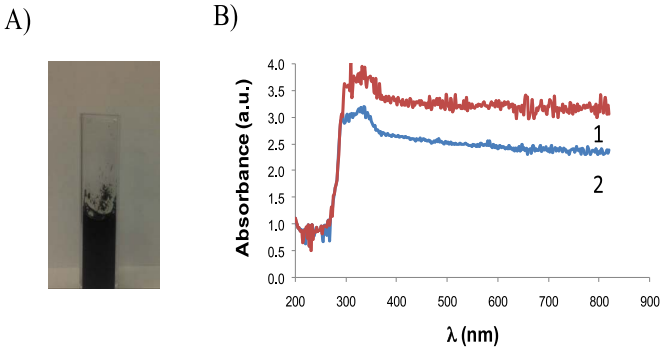

FIG. 11. — Water dispersion of CNT–SP (1 g/L): (A) after 2 wk storage at rest; (B) UV–Vis spectra: (1) after sonication and (2) after centrifugation.

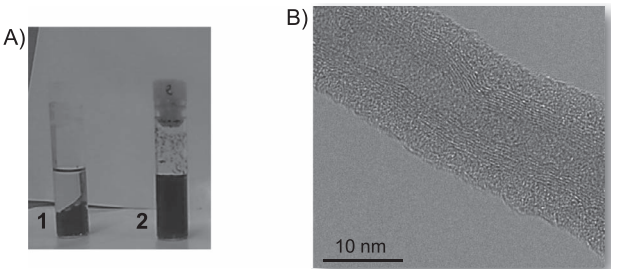

FIG. 12. — (A) Acetone suspensions of (1) CNT and (2) CNT–PU–SP after centrifugation at 5000 rpm for 5 min; (B) HRTEM micrograph of CNT–PU–SP adduct.

about 1530, 1395, 1490, and 802 cm^{-1}, due to the collective vibration mode of C=C/C–C stretching, reveal the presence of the pyrrole ring. Such bands are sort of fingerprint of SP.

The spectrum of HSAG–SP–T was taken on a sample extensively rinsed, as described in the "Experimental" section. This spectrum shows many bands that cannot be attributed to HSAG, typical of sp^3 C–H stretching, at about 2900 cm^{-1}; stretching of aromatic rings, in the region of C–C bonds, at 1590 and 1470 cm^{-1}; diol vibrations, at 1383 cm^{-1}; and vibration of the alkenyl groups absorbs, at 802 cm^{-1}. Moreover, in the HSAG–SP–T spectrum, there are bands absent in both HSAG and SP spectra, located at 1742 and 1662 cm^{-1}. They can be reasonably attributed to carbonyl groups, in particular to aldehydic and carboxyl group. It is also worth observing that the relative intensity of the peak at 802 cm^{-1}, due to the C=C stretching of the pyrrole ring, decreases in the spectrum of HSAG–SP–T adduct.

FT-IR analysis was also performed on CBN326-SP adduct. Spectra of HSAG–SP–T and CB–SP were collected in Figure 8b, to allow an easy comparison. They show similar features, although the HSAG-based adduct reveals more evident oxidation peaks.

WHAT ABOUT THE MECHANISM FOR ADDUCT FORMATION?

The characterization of SP adducts with carbon allotropes is as follows: (i) stable adducts are formed (functionalization yield was detected on thoroughly washed samples), (ii) bulk crystalline structure of graphitic substrate is substantially unaltered, (iii) SP is clearly visible in the adduct(s), in oxidized form.

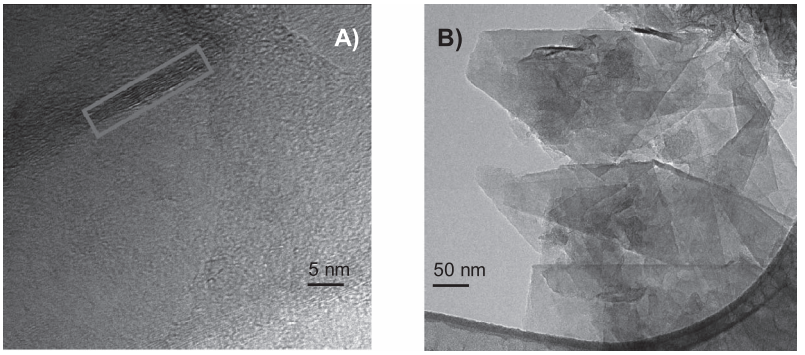

FIG. 13. — Micrographs of HSAG–SP–M adduct isolated from supernatant suspension, after centrifugation for 10 min at 2000 rpm: (A) HRTEM image; (B) low magnification bright field TEM.

TABLE IV
ADDUCTS OF SP WITH DIFFERENT CARBON ALLOTROPES YIELD OF FUNCTIONALIZATION[a]

Type of carbon allotrope	Commercial grade[b]	Surface area, m^2/g	Functionalization yield (%)	
			From TGA	From Soxhlet extraction
HSAG	Nano 24	353.2	91	91
GnP	Graphene Nano-platelets	750	95	94
CNT	Nanocyl 7000	275	n.d.[c]	94
CB	N326	77	n.d.[c]	90

[a] Calculated through Eq. 2.
[b] For commercial sources, see Experimental section.
[c] n.d. = not determined.

It was commented above that adduct preparation occurred at high temperatures and in the presence of air. Oxidation of the electron rich pyrrole ring can be thus assumed. It is also reasonable that such oxidation could occur on the lateral substituents of the pyrrole ring, the methyl groups. In fact, it is well known that the π–π interaction with a carbon allotrope protects an aromatic ring from oxidation.[94] Oxidation of the methyl group could justify the peak attributed to an aldehydic functionality. It can be thus assumed that the adduct is formed between the carbon allotrope and oxidized SP, which means a pyrrole ring with an electron withdrawing group at least in position 1 (there are not indications, at present, that both methyl groups of SP undergo oxidation). In the light of what is reported so far, it could be hypothesized as follows: SP is oxidized by air at high temperature, thanks to the presence of the carbon allotrope, which is indeed an oxidation catalyst.[95,96] Oxidized SP could give rise to a Diels–Alder reaction with the graphitic substrate. This reaction could justify the reduction of peak at 802 cm^{-1} in the IR spectrum, due to C=C bonds. Cycloaddition reaction already has been reported between graphene layers and dienophiles.[97–99] At present, such a mechanism should be taken with a pinch of salt. However, without stretching inferences too far, the following picture of the adduct of carbon allotropes with SP can be depicted: large unaltered surface of the graphitic material is available, and SP, tightly bonded, most likely in peripheral positions, brings the adduct into hydrophilic environments.

DISPERSIONS OF SP ADDUCTS WITH CARBON ALLOTROPES IN WATER AND ECO-FRIENDLY SOLVENTS

Adducts of carbon allotropes with SP were used to prepare stable dispersions in water and polymer latexes.

Water dispersions of HSAG were prepared in a wide range of concentrations: from 0.1 g/L to 200 g/L. Figure 9A shows dispersions, with concentrations from 0.1 g/L to 10 g/L, which were found to follow the Lambert–Beer law and to be stable at rest for weeks. Reduction of UV absorption of dispersion with 1 g/L concentration was observed only after centrifugation at 9000 rpm for 30 min.[80] High concentration dispersions were prepared in large quantities. Dispersions shown in Figure 9B have (a) 10, (b) 30, and (c) 50 g/L as concentrations: they show the increase of viscosity with the concentration.

Water dispersions were also prepared with CB N326, in concentration ranges from 0.01 g/L to 1 g/L. In Figure 10A, water dispersions of CB–SP (1 g/L) (1) and of CB (2) are shown: they were prepared by sonicating for 10 min, and centrifugation was then performed at 3000 rpm for 5 min. UV–Vis measurements were taken on the CB–SP dispersion, after sonication and centrifugation steps, without observing any difference.

TABLE V
AVERAGE SIZE OF HSAG–SP, CB–SP, CNT–SP IN WATER DISPERSIONS AND CNT–SP IN ETHYL ACETATE DISPERSION, DETERMINED THROUGH DLS

	Average size of particles (nm)	
Carbon allotrope[a]	Starting dispersion	Supernatant dispersion[b]
HSAG	300	150
CB N326	379	230
CNT	884	500
CNT[c]	140	50

[a] Functionalized with SP. Carbon allotrope/SP mass ratio = 10/1.
[b] After 30 min centrifugation at 9000 rpm.
[c] Dispersion in ethyl acetate.

Stable water dispersions were prepared as well with CNT. Figure 11A shows water dispersion with a CNT concentration of 1 g/L, and Figure 11B shows the moderate reduction of UV absorption upon centrifuging such dispersion at 9000 rpm for 5 min. CNT dispersions were visually observed to be less homogenous than the ones with CB and HSAG, at the same concentrations.

Dynamic light scattering analysis was performed, in spite of the limits of such investigation on carbonaceous materials, with the aim of comparing the average size of hydrodynamic radius of carbon allotrope particles in HSAG, CB, and CNT dispersions. Table V shows data of dispersions, immediately after sonication and taken as supernatant suspension after centrifugation at 9000 rpm for 30 min.

It appears that particles of HSAG–SP and CB–SP have lower average size than particles of CNT. The average size further decreases in the supernatant suspension. Low size was obtained also for CNT by preparing dispersions in an eco-friendly solvent such as ethyl acetate. It can be thus commented that functionalization with SP was not able, as such, to give rise to CNT disentanglement, and an organic environment was helpful for that. SP was used as comonomer in oligomers of polyurethanes (PU)[79] and polyethers (PE),[81] and very stable supramolecular interactions with CNT were obtained. Suspensions of CNT adducts with either PU or PE in acetone or ethyl acetate were stable for months, even after centrifugation: Figure 12 shows acetone suspensions of CNT and CNT–PU–SP after centrifugation at 5000 rpm for 5 min. CNTs isolated from the latter suspension were prevailingly disentangled and, as can be seen in Figure 12B, revealed in HRTEM pictures intact skeleton and SP-based oligomers tightly adhered to the CNT surface.

PREPARATION OF FEW LAYERS GRAPHENE

The previous paragraph showed that stable water suspensions are obtained with HSAG–SP. Through centrifugation of such suspensions at different rotations per minute, for different times, supernatant suspensions can be isolated. Few layers of graphene were isolated from such supernatant suspensions. Figure13A shows a stack, isolated from the supernatant suspension after centrifugation at 9000 rpm for 5 min, with 8 graphene layers. The lateral size of such layers, as shown in Figure 13B, is a few hundred nanometers and is substantially the same in pristine HSAG and in HSAG–SP from the supernatant suspension. Micrographs shown in Figure 13 are taken on HSAG–SP–M samples, which means samples prepared though milling. The combination of mechanical energy and SP is useful to obtain a few layers of graphene without breaking the layers.

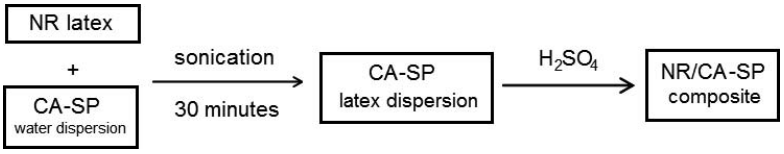

FIG. 14. — Procedure for the preparation of dispersions of a CA functionalized with serinol pyrrole in NR latex and of composite obtained therefrom.

DISPERSIONS OF SP ADDUCTS WITH CARBON ALLOTROPES IN NR LATEX

Dispersions of carbon allotropes in NR latex were prepared through the procedure shown in Figure 14. Suspensions of HSAG–SP in NR latex, shown in Figure 15A, were prepared with 10 phr of HSAG and were stable for weeks. Composites obtained by precipitation with H_2SO_4 revealed in TEM micrographs (see Figure 15B) only a few HSAG layers and isolated HSAG layers. In the WAXD pattern, shown in Figure 15C, the (002) reflection due to graphitic material hardly could be detected Also taking into account the low amount of HSAG in the composite, the preparation of HSAG–SP dispersion in NR latex promoted HSAG exfoliation.

Composites based on CBN326, obtained from latex dispersions through the procedure shown in Figure 14, revealed a very even and fine dispersion of CB particles. In Figure 16, TEM micrographs (at different magnifications) are shown for composites based on (A) CB and on (B) CB–SP. The latter composites did not reveal the presence of large CB agglomerates. CB particles were much finer and evenly dispersed.

IR/BR-BASED COMPOSITES WITH CB–SP AND CB AND SILICA AS THE FILLERS

Composites containing CB–SP were prepared, based on IR and BR as the rubbers and CB and silica as the fillers. The objective was to reduce the silica filler networking thanks to the silica interaction with functionalized CB. Recipes are shown in Table II in the "Experimental" section.

Two different levels of CB–SP were used, corresponding to 0.6 and 0.9 SP phr. In all composites, the same CB amount was used: SP was thus an extra ingredient in the compound. Cross-linking was performed with a sulfur-based system.

Rheometric curves, taken at 170 °C and shown in Figure 17, do not reveal appreciable differences of vulcanization kinetic: induction times (t_{s1}) (t_{90}) were found to be very similar. Treatment with SP does not modify the surface properties of CB. This could be expected considering the experimental conditions for the preparation of the adducts. However, in addition to

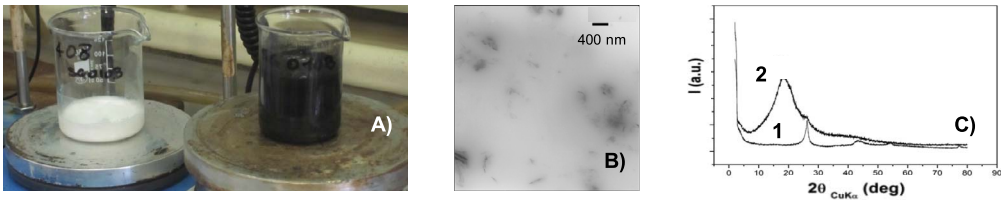

FIG. 15. — (A) NR latex and suspension of HSAG–SP in NR latex; (B) TEM micrograph of composite obtained from such dispersion (see Figure 14); (C) WAXD pattern of the composite: (1) HSAG–SP, (2) composite.

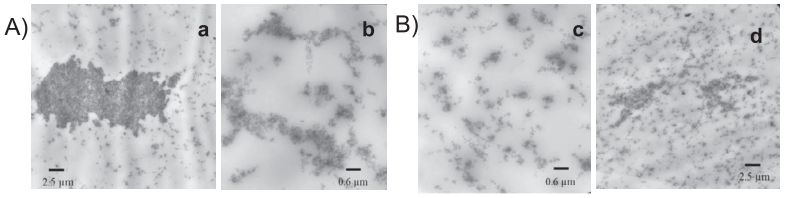

FIG. 16. — TEM micrographs of NR-based composites containing: (A) CB; (B) CB–SP.

the hydroxy groups, to CB is added a basic nitrogen, which could promote a faster vulcanization. At the explored SP level, this is not observed. The use of CB–SP leads to slightly lower levels of M_H.

To investigate filler networking phenomenon, strain sweep experiments were performed at 50 °C, on cross-linked samples. The dependence of shear storage modulus G' as a function of strain amplitudes is shown in Figure 18A, and the dependence of shear loss modulus G'' as a function of G' is shown in Figure 18B. The addition of CB–SP leads to the reduction of the Payne Effect.[100,101] As it appears from the Cole–Cole plot in Figure 19, for a given level of dynamic stiffness, the use of CB–SP shows lower loss modulus.

NR-BASED COMPOSITES WITH CB–SP AND CB AS THE FILLER

CB–SP was also used in a composite based on NR as the rubber and CB as the only filler. The objective of this experiment was to verify if SP can promote the reduction of filler networking of CB, thanks to the interaction of hydroxy groups on the CB surface with silanols of a sulfur-based silane such as bis[3-(triethoxysilyl)propyl]tetrasulfide (TESPT). The formulation was very simple indeed (it is reported in Table III in the "Experimental" section): the composite contained only NR and CB (100 and 50 phr, respectively) and was cross-linked with sulfur, in the absence and in the presence of TESPT. Strain sweep experiments were carried out on the cross-linked composites, at 50 °C. G' dependence on strain amplitude is in Figure 19A: the combination of CB–SP with TESPT brings about the reduction of Payne effect. It is worth commenting on the cross-over of the curves, which could mean that SP can promote a bond between CB and the poly(isoprene) chain. To justify such assumption, the hypothesized cycloaddition reaction between SP and the carbon allotrope may

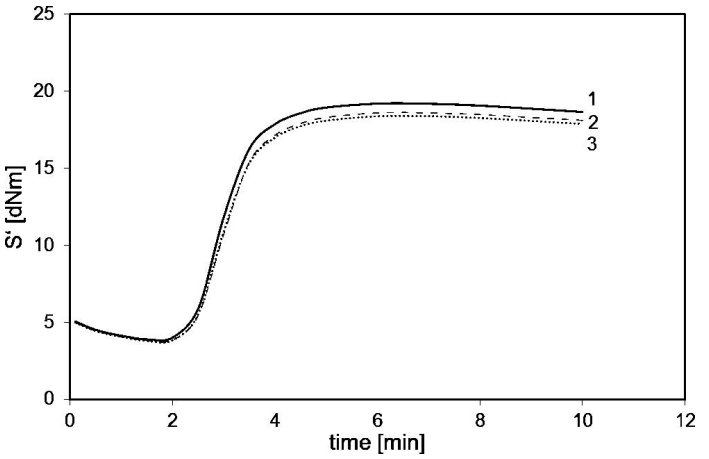

FIG. 17. — Rheometric curves obtained at 170 °C for composites of Table II containing different amounts of CB–SP: (1) 0 phr; (2) 5 phr; (3) 7.5 phr.

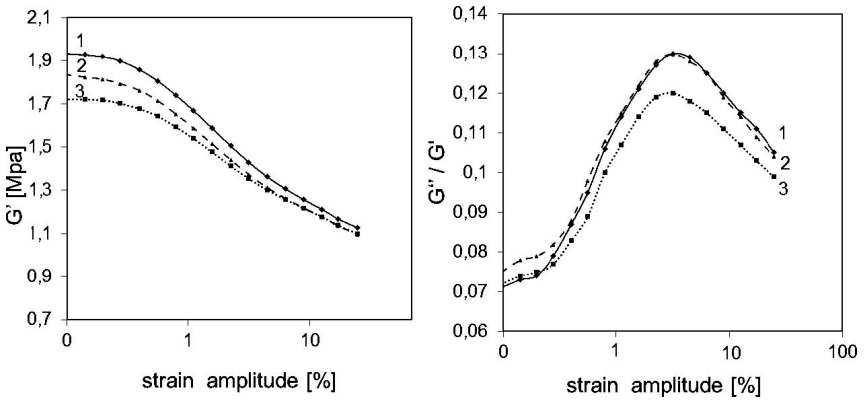

FIG. 18. — (A) Dynamic storage modulus G' (MPa) vs strain amplitude (%) and (B) loss modulus G'' vs G' for cross-linked composites of Table II. The content of CB–SP was (1) 0 phr; (2) 5 phr; (3) 7.5 phr.

form a double bond in the adduct. The Cole–Cole plot in Figure 19B indicates that lower loss modulus is obtained for a given dynamic stiffness.

CONCLUSIONS

This work demonstrates that it is possible to functionalize sp^2 carbon allotropes, both nano-size and nano-structured, using the same molecule and introducing oxygenated functional groups through a soft chemistry synthetic route, leaving substantially unaltered the bulk crystalline structure of the graphitic materials.

A serinol derivative was used as the molecule for functionalization: 2-(2,5-dimethyl-1*H*-pyrrol-1-yl)-1,3-propanediol. Such a molecule, which can be also obtained from renewable sources, comes from glycerol as the starting building block. Glycerol has long been investigated for the development of a C-3 platform alternative to the oil-based one. This work thus adds a further perspective for this inexpensive and environmentally friendly chemical.

Multiwalled CNT, nano-sized graphites with high surface area, and different grades of carbon black were used as the carbonaceous materials. By simply mixing them with serinol pyrrole and using either thermal or mechanical energy, functionalization occurred with high yield, in all cases larger than 90%.

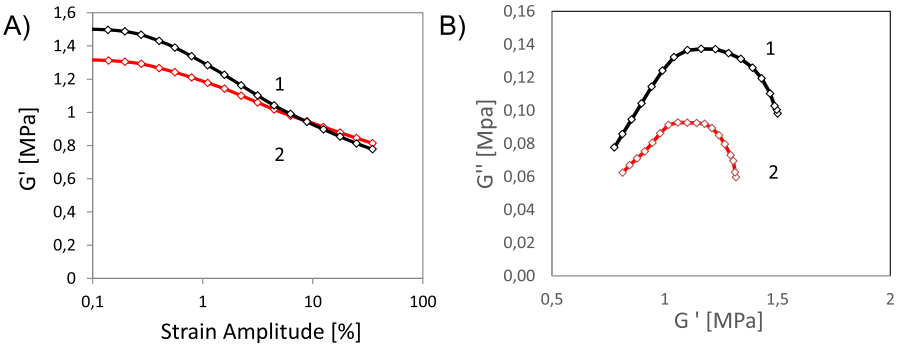

FIG. 19. — (A) Dynamic storage modulus G' vs strain amplitude and (B) loss modulus G'' vs strain amplitude for cross-linked composites of Table III.

Experimental findings suggest that covalent bonds are formed between SP and the aromatic substrate through a cycloaddition reaction. Modification occurs in peripheral positions of the carbon material, which substantially maintains their properties.

The hydroxy group on the carbon surface allowed the preparation of stable dispersions of the carbon allotropes in water and in NR latex. Composites obtained from latex dispersions revealed nanometric carbon particles very evenly distributed.

It was found that the CB adduct with SP is able to promote the reduction of the Payne effect in compounds based on either CB or CB and silica as the fillers and cross-linked with sulfur-based systems.

In the "Introduction" it is noted that common features can be identified for both nano-size and nano-structured sp^2 carbon allotropes, able to commonly describe their behavior in mechanical reinforcement and sulfur-based cross-linking. In this manuscript, a common functionalization technology has been presented. This work paves the way for the use of bio-sourced chemicals for tuning the solubility parameters of sp^2 carbon allotropes without altering their precious and highly desired properties.

REFERENCES

[1]C. Goodyear, *Gum-Elastic and Its Varieties: With a Detailed Account of Its Applications and Uses, and of the Discovery of Vulcanization*, New Haven, CT, 1853.

[2]J. B. Donnet and E. Custodero, "Reinforcement of Elastomers by Particulate Fillers," in *The Science and Technology of Rubber,* 3rd ed., J. E. Mark, B. Erman, and F. R. Eirich, Eds., Academic Press, San Diego, 2005.

[3]M. Gerspacher and W. Wampler, *Basic Elastomer Technology*, Vol. 57, ACS, Washington, DC, 2001.

[4]M. J. Wang, C. A. Gray, S. A. Reznek, K. Mahmud, and Y. Kutsovsky, "Carbon Black," in *Kirk-Othmer Encyclopedia of Chemical Technology*, Wiley, New York, 2003.

[5]A. Voet, J. C. Morawski, and J. B. Donnet, RUBBER CHEM. TECHNOL. **50**, 342 (1977).

[6]M. Maiti, M. Bhattacharya, and A. K. Bhowmick, RUBBER CHEM. TECHNOL. **81**, 384 (2008).

[7]D. R. Paul and L. M. Robeson, *Polymer* **49**, 3187 (2008).

[8]M. Galimberti, V. Cipolletti, S. Musto, S. Cioppa, G. Peli, M. Mauro, G. Guerra, S. Agnelli, T. Riccò, and V. Kumar, RUBBER CHEM. TECHNOL. **87**, 417 (2014).

[9]M. Galimberti, V. Cipolletti, and V. Kumar, "Natural Rubber Materials: Volume 2: Composites and Nanocomposites," S. Thomas, C.H. Chan, L. Pothan, J. Joy, H. Maria, Eds., Royal Society of Chemistry, London, 2013, Ch. 2.

[10]M. Galimberti, *Rubber Clay Nanocomposites: Science, Technology, Applications*, John Wiley and Sons, 2011.

[11]M. Galimberti, *Advanced Elastomers – Technology, Properties and Applications*, A. Boczkowska, Ed., InTech, Rijeka, Croatia, 2012, Ch. 4.

[12]M. Galimberti, V. Cipolletti, and M. Coombs, *Handbook of Clay Science* **4.4** (2013)

[13]L. Bokobza. *Polymer* **48**, 4907 (2007).

[14]M. Bhattacharya, M. Maiti, and A. K. Bhowmick, *Polym. Eng. Sci.* **49**, 81 (2009).

[15]A. K. Bhowmick, M. Bhattacharya, and S. Mitra, *J. Elastomers Plastics* **42**, 517 (2010).

[16]F.R. Al-Solamya, A. A. Al-Ghamdib, and W. E., Mahmou, *Polym. Adv. Technol.* **23**, 478 (2012).

[17]M. Galimberti, V. Kumar, M. Coombs, V. Cipolletti, S. Agnelli, S. Pandini, and L. Conzatti, RUBBER CHEM. TECHNOL. **87**, 197 (2014).

[18]M. Galimberti, S. Agnelli, and V. Cipolletti, "Hybrid filler systems in rubber nanocomposites," in S. Thomas and H. Maria, Eds., *Progress in Rubber Nanocomposites*, 1st ed., Woodhead Publishing, Sawston, Cambridge, UK, 2017.

[19]M. Terrones, A. R. Botello-Méndez, J. Campos-Delgado, F. López-Urías, Y. I. Vega-Cantú, F. J. Rodríguez-Macías, and H. Terrones, *Nano Today*. **5**, 351 (2010)

[20]J. Zhang, M. Terrones, C. R. Park, R. Mukherjee, M. Monthioux, N. Koratkar, Y. S. Kim, R. Hurt, E. Frackowiak, T. Enoki, Y. Chen, Y. S. Chen, and A. Bianco, *Carbon* **98**, 708 (2016).

[21]M. Mauro, V. Cipolletti, M. Galimberti, P. Longo, and G. Guerra, *J. Phys. Chem. C* **116**, 24809 (2012).

[22]S. Agnelli, V. Cipolletti, S. Musto, M. Coombs, L. Conzatti, S. Pandini, T. Riccò, and M. Galimberti, *eXPRESS Polymer Letters* **8**, 436 (2014).

[23]U. Szeluga, B. Kumanek, and B. Trzebicka, *Composites: Part A* **73**, 204 (2015).

[24]M. Galimberti , M. Coombs, P. Riccio, T. Ricco, S. Passera, S. Pandini, L. Conzatti, A. Ravasio, and I. Tritto, *Macromol. Mater. Eng*. **298**, 241 (2012),

[25]B. Dong, C. Liu, Y. Lu, and Y. Wu, *J. Appl. Polym. Sci*. **132**, 42075 (2015).

[26]S. Musto, V. Barbera, V. Cipolletti, A. Citterio, and M. Galimberti, *eXPRESS Polymer Lett*. **11**, (6), 435–448.

[27]P. Singh, S. Campidelli, S. Giordani, D. Bonifazi, A. Bianco, and M. Prato, *Chem. Soc. Rev*. **38**, 2214 (2009).

[28]M. Rahmat and P. Hubert, *Carbon, Composites Sci. Technol*. **72**, 72, (2011).

[29]P. Bilalis, D. Katsigiannopoulos, A. Avgeropoulos, and G. Sakellariou, *RSC Advances* **4**, 2911 (2014).

[30]K. Subramaniam, A. Das, and G. Heinrich, *Composites Sci. Technol*. **71**, 1441, (2011).

[31]H. Yang, F. Li, C. Shan, D. Han, Q. Zhang, L. Niu, and A. Ivaskab, *J. Mater. Chem*. **19**, 4632, (2009).

[32]T. M. Swager, *ACS Macro Lett*. **1**, 3 (2012).

[33]I. Zaman, H. C. Kuan, Q. Meng, A. Michelmore, N. Kawashima, T. Pitt, L. Zhang, S. Gouda, L. Luong, and J. Ma, *Adv. Funct. Mater*. **22**, 2735 (2012).

[34]C. K. Chua and M. Pumera, *Chem. Soc. Rev*. **42**, 3222 (2013).

[35]D. Bhattacharjya, I. Y. Jeon, H. Y. Park, T. Panja, J. BeomBaek, and J. S. Yu, *Langmuir* **31**, 5676 (2015).

[36]P. Xiong, J. Zhu, L. Zhang, and X. Wang, *Nanoscale Horiz.* **1**, 340 (2016).

[37]A. Kausar, Z. Anwar, L.A. Khan, and B. Muhammad, *Fullerenes Nanotubes Carbon Nanostruct*. **25**, 47 (2017).

[38]Y. Luo, P. Zhao, Q. Yang, D. He, L. Kong, and Z. Peng, *Compos. Sci. Technol*. **100**, 143 (2014)

[39]J. R. Potts, O. Shankar, L. Du, and R. S. Ruoff, *Macromolecules* **45**, 6045 (2012).

[40]J. B. Donnet, R. C. Bansal, and M. J. Wang, *Carbon Black: Science and Technology*, Marcel Dekker, New York, 1993.

[41]M. J. Wang, Y. Kutsovsky, P. Zhang, L. J. Murphy, S. Laube, and K. Mahmud, RUBBER CHEM. TECHNOL. **75**, 247 (2002).

[42]M. J. Wang, K. Mahmud, L. J Murphy, & W. J. Patterson, *Kautschuk Gummi Kunststoffe* **51**, 348 (1998).

[43]W. Wang, A. Vidal, J. B. Donnet, and M. J. Wang, *Kautschuk Gummi Kunststoffe* **46,** 933 (1993).

[44]C. R. Kinney and L. D. Friedman, *J. Am. Chem. Soc*. **57**, 74 (1952).

[45]M. R. Cines, U.S. Patent 2,692,227 (to Phillips Petroleum Co.), October 19, 1954.

[46]F. Cataldo, *J. Nanosci. Nanotechnol*. **7**, 1446 (2007).

[47]J. A. Belmont, V. R. Tirumala, and P. Zhang, PCT Application WO 2013130099, 2013.

[48]W. Wampler, B. M. Jacobsson, L. Nikiel, P. D. Cameron, and J. Neilsen, U.S. Patent 20150191579 (to Sid Richardson Carbon Ltd.), July 9, 2015.

[49]B. C. Brodie, *Philos. Trans. R. Soc. Lond.* **14**, 249 (1859).

[50]L. Staudenmaier, *Ber. Dtsch. Chem. Ges*. **31,** 1481 (1898).

[51]W. S. Hummers and R. E. Offeman, *J. Am. Chem. Soc*. **80**, 1339 (1958).

[52]D. C. Marcano, D. V. Kosynkin, J. M. Berlin, A. Sinitskii, Z. Sun, A. Slesarev, L. B. Alemany, W. Lu, and J. M. Tour, *ACS Nano*. **4**, 4806 (2010).

[53]J. Chen, B. Yao, C. Li, and G. Shi, *Carbon* **64**, 225 (2013).

[54]J. Chen, Y. Li, L. Huang, C. Li, and G. Shi, *Carbon* **81,** 826 (2015).

[55]J. Guerrero-Contreras and F. Caballero-Briones, *Mater. Chem. Phys*. **153**, 209 (2015).

[56]N. I. Kovtyukhova, P. J. Ollivier, B. R. Martin, T. E. Mallouk, S. A. Chizhik, E. V. Buzaneva, and A. D. Gorchinskiy, *Chem. Mater*. **11**, 771 (1999).

[57]O. Yu. Posudievsky, O. A. Khazieieva, V. G. Koshechko, and V. D. Pokhodenko, *J. Mater. Chem.* **22**, 12465 (2012).

[58]H. P. Boehm, A. Clauss, G. O. Fischer, and U. Hofmann, *Z. Naturforsch Pt. B*. **17**, 150 (1962).

[59]G. Eda, G. Fanchini, and M. Chhowalla, *Nat. Nanotechnol*. **3**, 270 (2008).

[60]C. Gomez-Navarro, R. T. Weitz, A. M. Bittner, M. Scolari, A. Mews, M. Burghard, and K. Kern, *Nano Lett*. **7**, 3499 (2007).

[61]S. Stankovich, D. A. Dikin, R. D. Piner, K. A. Kohlhaas, A. Kleinhammes, Y. Jia, Y. Wu, S. T. Nguyen, and R S. Ruoff, *Carbon* **45**, 1558 (2007).

[62]X. B. Fan, W. Peng, Y. Li, X. Li, S. Wang, G. Zhang, and F. Zhang, *Adv. Mater*. **20**, 4490 (2008).

[63]S. Abdolhosseinzadeh, H. Asgharzadeh, and H. S. Kimb, *Sci. Rep*. **5**, 10160 (2015).

[64]D. Li, M. B. Muller, S. Gilje, R. B. Kaner, and G. G. Wallace, *Nat. Nano*. **3**, 101 (2008).

[65]S. Stankovich, D. A. Dikin, G. H. B. Dommett, K. M. Kohlhaas, E. J. Zimney, E. A. Stach, R. D. Piner, S. T. Nguyen, and R. S. Ruoff, *Nature* **442**, 282 (2006).

[66]F. You, D. Wang, J. Cao, X. Li, Z.-M. Dang, and G.-H. Hu, *Polym. Int*. **63**, 93 (2014).

[67]L. J. Cote, R. Cruz-Silva, and J. Huang, *J. Am. Chem. Soc*. **131**, 11027 (2009).

[68]M. Mauro, V. Cipolletti, M. Galimberti, P. Longo, and G. Guerra, *J. Phys. Chem. C* **116**, 24809 (2012).

[69]Y. Hernandez, S. Pang, X. Feng, and K. Müllen, *Polym. Sci.: Comprehensive Ref*. **8**, 415 (2012).

[70]C. A. Quispe, C. J. Coronado, and J. A. Carvalho Jr., *Renewable Sustainable Energy Rev*. **27**, 475 (2013).

[71]L. T. Thanh, K. Okitsu, L. V. Boi, and Y. Maeda, *Catalysts* **2**, 191 (2012)

[72]F. Yang, M. A. Hanna, and R. Sun, *Biotechnol. Biofuels* **5**, 1 (2012).

[73]B. Andreeßen and A. Steinbüchel, *AMB Express* **1**, 1 (2011).

[74]M. Galimberti, V. Barbera, A. Citterio, R. Sebastiano, A. M. Valerio, and G. Leonardi, PCT application WO 2015EP72641, 2015.

[75]V. Barbera, A. Porta, L. Brambilla, S. Guerra, A. Serafini, A. M. Valerio, and M. Galimberti, *RSC Adv*. **6**, 87767 (2016).

[76]L. Knorr, *Chem. Ber*. **18**, 299 (1885).

[77]C. Paal, *Chem. Ber*. **18**, 367 (1885).

[78]V. Barbera, A. Citterio, M. Galimberti, G. Leonardi, R. Sebastiano, S. U. Shisodia, and A. M. Valerio, PCT application WO 2015189411, 2015.

[79]M. Galimberti, V. Barbera, A. Citterio, R. Sebastiano, A. Truscello, A. M. Valerio, L. Conzatti, and R. Mendichi, *Polymer* **63**, 62 (2015).

[80]M. Galimberti, V. Barbera, S. Guerra, L. Conzatti, C. Castiglioni, L. Brambilla, and A. Serafini, *RSC Adv*. **5**, 81142 (2015).

[81]V. Barbera, S. Musto, A. Citterio, L. Conzatti, M. Galimberti, *Express Polym. Lett*. **10**, 548 (2016).

[82]H. S. Broadbent, W. S. Burnham, R. M. Sheeley, and R. K. Olsen, *J. Heterocyclic Chem*. **13**, 337 (1976).

[83]C. Casagrande, P. Fabre, M. Veyssie, and E. Raphael, *Europhysics Lett. (EPL)* **9**, 251 (1989).

[84]P. G. de Gennes, *Angewandte Chem. Int. Ed*. **31**, 842 (1992).

[85]F. Li, D. P. Josephson, and A. Stein, *Angewandte Chem. Int. Ed*. **50**, 360 (2011).

[86]H. Mori and A. H. Müller, *Prog. Polym. Sci*. **28**, 1403 (2003).

[87]R. Ricciarelli, J. M. Zingg, and A. Azzi, *The FASEB J*. **15**, 2314 (2001).

[88]C. Castiglioni, M. Tommasini, and G. Zerbi, *Philos. Trans. Roy. Soc. Lond. A* **362**, 2425 (2004).

[89]L.R. Radovic and B. Bockrath, *J. Am. Chem. Soc*. **127**, 5517 (2005).

[90]A. C. Ferrari, J. C. Meyer, V. Scardaci, C. Casiraghi, M. Lazzeri, F. Mauri, and A. K. Geim, *Phys. Rev. Lett*. **97**, 187401 (2006)

[91]D. Graf, F. Molitor, K. Ensslin, C. Stampfer, A. Jungen, C. Hierold, and L. Wirtz, *Nano Lett*. **7**, 238 (2007).

[92]C. Casiraghi, A. Hartschuh, H. Qian, S. Piscanec, C. Georgi, A. Fasoli, K. S. Novoselov, D. M. Basko, and A. C. Ferrari, *Nano Lett*. **9**, 1433 (2009).

[93]M. Tommasini, C. Castiglioni, G. Zerbi, A. Barbon, and M. Brustolon, *Chem. Phys. Lett*. **516**, 220 (2011).

[94]S. Navalon, A. Dhakshinamoorthy, M. Alvaro, and H. Garcia. *Chem. Rev*. **114**, 6179 (2014).

[95]C. K. Chua and M. Pumera, *Chem. Eur. J*. **21**, 12550 (2015).

[96]J. W. To, J. W. D. Ng, S. Siahrostami, A. L. Koh, Y. Lee, Z. Chen, K. D. Fong, S. Chen, J. He, W.-G. Bae, J. Wilcox, H. Y. Jeong, K. Kim, F. Studt, J. K. Nrskov, T. F. Jaramillo, and Z. Bao, *Nano Res*. **10**, 1163 (2017).

[97]L. Daukiya, C. Mattioli, D. Aubel, S. Hajjar-Garreau, F. Vonau, E. Denys, G. Reiter, J. Fransson, E. Perrin, M.-L. Bocquet, C. Bena, A. Gourdon, and L. Simon, *ACS Nano* **11**, 627 (2017).

[98]S. Sarkar, E. Bekyarova, S. Niyogi, and R. C. Haddon, *J. Am. Chem. Soc*. **133**, 3324 (2011).

[99]S. Sarkar, E. Bekyarova, and R. C. Haddon, *Accounts Chem. Res*. **45**, 673 (2012).

[100]A. R. Payne and R. E. Whittaker, RUBBER CHEM. TECHNOL. **44**, 440 (1971).

[101]A. R. Payne, "Dynamic Properties of Filler-Loaded Rubbers," in *Reinforcement of Elastomers*, G. Kraus Ed., Interscience Publishers, New York, London, Sydney, 1965, pp. 69–114.

[*Received March 2017; Revised June 2017*]